Semester Thesis - Qubit Simulation And Design

Adrian Ryser
Spring Semester 2014

Supervisor: Dr. Mintu Mondal

ETH Zurich
Quantum Device Lab
Prof. Dr. A. Wallraff

Abstract

Quantum circuits based on superconducting qubits are one of the most promising candidates for scalable quantum information processing. However the performance of superconducting qubits is limited by energy relaxation and low coherence times. To understand the underlying decay mechanisms which limit the relaxation time, a complete circuit model of the qubit and its control circuitry was studied. Our circuit model indicates two dominant decay channels which are responsible for the observed energy relaxation time in our present device. In order to minimize the design specific decay processes a new design is proposed. Based on a simulation study of our model the energy relaxation time of this new design is expected to be higher by a factor of 2-3.

Contents

1   Introduction

Over the last few decades the fields of quantum information and quantum computing have grown significantly both on the theoretical and on the experimental side [1]. This fast progress has resulted in new quantum algorithms which solve certain problems like prime factoring [2] or searching in an unsorted database [3] more efficiently than classical algorithms. Although these algorithms have been implemented in recent years on experimental systems using a small number of qubits and gates [4, 5], it will still take considerable time and effort to develop the future quantum computer which will eventually solve problems we cannot solve (equally fast) on a classical computer. Another promising application is the simulation of quantum systems which are hard to simulate on a classical computer because of the exponential growth of the Hilbert space with problem size [1].

A wide range of different systems have been pursued as quantum bits (qubits) including superconducting qubits [6], trapped ions [7] and photons [8], but no particular system has emerged as a clear leader yet. Important requirements that a qubit in a future quantum computer has to fulfill are long decoherence times, reliable control and up-scalability.

Great progress has been achieved recently on these issues using superconducting qubits. Anyhow decoherence times in these systems are still limited in the best case to the few ten microsecond range [9]. Our transmon qubits, a type of superconducting qubits, achieve maximal lifetimes of about 6 μs. The implementation of error correction schemes or generally more complex algorithms using a large number of gates still needs longer energy relaxation times. In order to reach higher relaxation times it is essential to understand the limiting factors. In recent years a vast amount of possible decay mechanisms have been presented [10]. In practice it is not obvious which decay mechanisms are actually limiting the energy relaxation time for the qubits in use. The main goal of this semester thesis was to develop a circuit model which simulates the qubit and the control circuitry used to operate and manipulate the qubit. Such a model can then be used to understand the contribution of certain decay channels to the total decay rate. With the help of the gained information, new qubits can be designed to minimize the influence of design specific decay channels.

2 Theory

2.1 Transmon

The following section gives a short overview of the transmon qubit and its theoretical description closely following Ref. [10].

The qubit type used in this group is a superconducting charge qubit called transmon. A schematic of a transmon qubit and equivalent electric circuit are shown in Figures 1a and 1b respectively. The qubit is based on two superconductors called island and reservoir which are connected over two Josephson junctions [11] forming a SQUID-loop. The two Josephson junctions allow Cooper pairs to tunnel from the island to the reservoir and back. The Hamiltonian describing the system is given by

$$\hat{H} = 4E_C \left(\hat{n} - n_g\right)^2 - E_J \cos \hat{\varphi}$$

where $\hat{n}$ describes the number of Cooper pairs tunneled from one island to the other and $\hat{\varphi}$ is the phase difference between the two superconductors. The parameter $n_g = Q_r/2e + C_g V_g/2e$ describes the offset charge measured in units of Cooper-pairs due to environment-induced charges (first term) and an applied gate voltage (second term). The charging energy $E_c = e^2/2C_\Sigma$ $(C_\Sigma = C_B + C_J + C_g)$ is the energy needed to add an additional electron to the island. The Josephson energy E_J is the potential energy stored in the Josephson junction and can be tuned by the magnetic flux Φ threading through the SQUID-loop,

$$E_J(\Phi) = E_{J_{\max}} \left| \cos \left(\frac{\pi \Phi}{\Phi_0} \right) \right|$$

where $E_{J_{\max}}$ is determined by fabrication details and geometry of the Josephson junctions and Φ_0 is the flux quantum. Due to the fact that the dependence of the eigenenergies on n_g decays exponentially with the ratio E_J/E_C, the transmon is operated in the regime where $E_J/E_C >> 1$. In this approximation the eigenenergies of the above Hamiltonian can be analytically calculated using perturbation theory

$$E_m \approx -E_J + \sqrt{8E_C E_J} \left(m + \frac{1}{2} \right) - \frac{E_C}{12} \left(6m^2 + 6m + 3 \right).$$

The absolute anharmonicity $(= \Delta_{m+1} - \Delta_m, \; \Delta_m = E_m - E_{m-1})$ for the energy spectrum is $-E_C$. The energy levels are (in the approximation stated above) independent of n_g which significantly reduces the influence of charge noise on the energy spectrum which is needed for a qubit with a fixed transition energy. The lowest two levels (m=0, m=1) are used as the ground and the excited state of the transmon qubit. The anharmonicity of the spectrum ensures that the qubit is not excited to higher states than the first excited state.
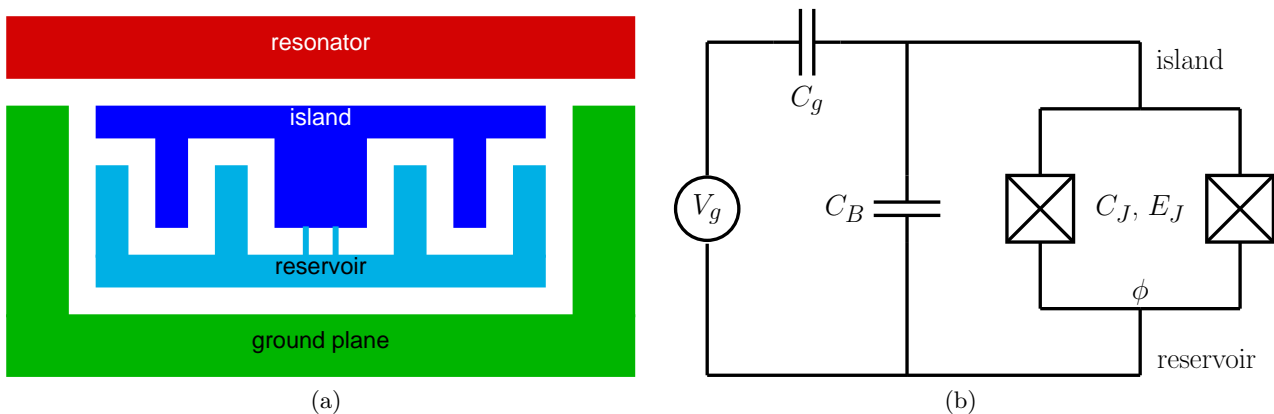
Figure 1: (a) Schematic of transmon qubit which consists of two superconductors island and reservoir connected by two Josephson junctions. The neighboring coplanar waveguide resonator is used for the state readout of the qubit. (b) Equivalent circuit of transmon qubit and resonator. The qubit is coupled over the capacitance C_g to the resonator whose electrical potential can be adjusted by the voltage V_g. The capacitance C_B represents the additional capacitance, besides the junction capacitance C_J, between island and reservoir due to the "fingers". (source: Ref. [16])

2.2 Jaynes-Cummings model for qubit coupled to resonator

In order to use the transmon as a functional qubit, there have to be means to readout and manipulate the state of the qubit. For the state readout a coplanar waveguide resonator placed nearby the qubit is used (see Figure 1a). Hence the transmon is capacitively coupled to the resonator and the total system can be described by the Jaynes-Cummings Hamiltonian

$$\hat{H} = \hbar \sum_i \omega_i \left|i\right\rangle\left\langle i\right| + \hbar\omega_r a^\dagger a + \hbar \sum_{i,j} g_{ij} \left|i\right\rangle\left\langle j\right| (a + a^\dagger).$$

The first term describes the transmon, where $\left|i\right\rangle$ is an energy eigenstate and $\hbar\omega_i$ the corresponding energy. The second term represents the resonator in the approximation that only one fundamental mode with resonance frequency ω_r is present and $a^\dagger, a$ are the creation and annihilation operators for resonator excitations. The third term describes the interaction between the qubit and the resonator eigenstates with couplings

$$g_{i,j} = \frac{2e}{\hbar} \frac{C_g}{C_\Sigma} \sqrt{\frac{\hbar\omega_r}{2C_r}} \left\langle i \left| n \right| j \right\rangle$$

and $C_r = \pi/(2\omega_r Z_0)$, $Z_0 = 50\,\Omega$. Using the rotating wave approximation and considering only the two lowest transmon levels the Hamiltonian reduces to

$$\hat{H} = -\frac{\hbar\omega_q}{2}\sigma^z + \hbar\omega_r \left(a^\dagger a + \frac{1}{2}\right) + \hbar g \left(a^\dagger \sigma^- + a\sigma^+\right)$$

with $\omega_q = \omega_0$, $g = g_{01}$ and σ^z the third Pauli-matrix. The operators σ^+, σ^- are the ladder operators for the two qubit state and given by the two Pauli-matrices σ^x, σ^y,

$$\sigma^+ = \sigma^x + i\sigma^y, \quad \sigma^- = \sigma^x - i\sigma^y.$$

3 Qubit relaxation

If the qubit is prepared in the excited state it will eventually decay into the ground state after some finite time due to its coupling to the environment. This can either be the control circuit used to manipulate and measure the state of the qubit or some additional decay channels like the host substrate. The main goal of designing a qubit is to minimize decay due to the control circuit while at the same time maintaining optimal control of the qubit. The total decay rate of the qubit is given by the sum of all individual decay rates due to different channels

$$\Gamma^{tot} = \sum_i \Gamma^i.$$

The energy relaxation time of the qubit is given by

$$T_1 = \frac{1}{\Gamma^{tot}}.$$

Few known important decay channels which limit T_1 time, are discussed below.

3.1 Purcell decay

If a two level system is placed inside a resonator the decay rate from the excited to the ground state is enhanced if system and resonator are in resonance and reduced if they are off-resonance, compared to the case that the two-level system is coupled to the vacuum [12]. The same effect occurs for a transmon qubit coupled to a coplanar wave guide resonator [13]. In the approximation that the qubit is coupled to the lowest photonic mode of the resonator and its frequency being close to the resonator frequency the spontaneous decay rate from the first excited state to the ground state is increased by the Purcell rate [10]

$$\Gamma_{(0,1)}^{Purcell} = \kappa \frac{g_{01}^2}{\Delta_0^2}$$

where $1/\kappa$ is the cavity lifetime, g_{01} the coupling of the qubit to the photonic mode and $\Delta_0 = \omega_r - \omega_q$ the detuning of the qubit to the resonator.

3.2 Coupling to flux line

The qubit is inductively coupled to the flux line. First the SQUID-loop couples with a mutual inductance M to the flux line. This coupling allows to tune the qubit frequency by changing the magnetic flux threading through the SQUID by varying the flux line current. Thus this intentional coupling is maximized in the qubit design process in order to have a good control over the qubit frequency. Secondly the whole qubit circuit couples with the mutual inductance M' to the flux line. Both couplings introduce additional decay channels, visualized in Figure 2.

In the first case current noise in the flux line leads to a fluctuating magnetic flux seen by the SQUID through the mutual inductance M, which can eventually lead to qubit relaxation.

Figure 2: Simplified schematic of qubit modelled as LC-oscillator and inductively coupled to the flux line. (source: Ref. [10])

In the second case one can consider the qubit as a classical LC-circuit with $L \approx \hbar^2/(4e^2 E_J)$ and $C \approx e^2/(2E_C)$ which is inductively coupled to the flux line. The charge oscillates between island and reservoir as $Q(t) = Q_0 \cos(\omega t)$ with frequency $\omega = 1/\sqrt{LC}$. The current is also time dependent and given by $I(t) = -I_0 \sin(\omega t)$ with $I_0 = \omega\sqrt{2C\hbar\omega}$. This oscillating current induces over the mutual inductance M' a voltage $V(t) = V_0 \sin(\omega t)$ and a corresponding current in the flux line. Due to the finite resistance of the flux line energy is dissipated and qubit relaxation may occur [10].
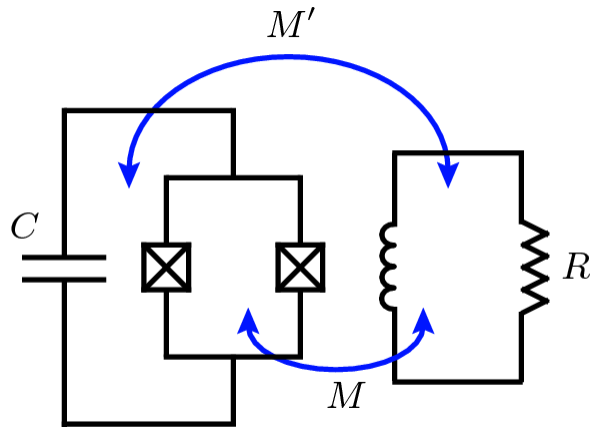
3.3 Dielectric loss

There are a number of internal decay channels which are gathered under the term dielectric loss. Generally the idea is that two level systems (TLS) which reside in the bulk substrate or at interfaces have an electric dipole moment over which they couple to the electric fields associated with the qubit. Energy can be exchanged and dissipated trough these TLS [14]. The TLS may be due to impurities in the substrate (in the bulk or the insulating layer of the Josephson junction) or oxides forming at exposed surfaces. The density and the individual contribution of different types of TLS to energy relaxation remains an active area of research. Here we model overall dielectric loss as the dielectric loss of the sapphire wafer. The internal loss of electromagnetic energy (e.g. into heat) is quantified by the dielectric loss tangent $\tan(\delta)$ [15]. The decay rate of the qubit due to dielectric loss is expected to be proportional to the loss tangent of the substrate material.

3.4 Other decay channels

In addition to the processes described above there are other decay channels like the charge line, spurious PCB modes or quasiparticle tunneling [10]. Decay to charge line seems not to be a limiting factor of T_1 as simple calculations [16] show. We also think that the other additional decay channels do not currently limit T_1 as our model suggests, which includes the first three decay mechanisms.

4 Complete model of qubit and its control circuitry

The main goal of this semester thesis was to develop a quantitative model to estimate the energy relaxation time of the qubits in use. This was achieved by simulating the qubit and its environment (resonator, flux- and charge line) as a classical microwave circuit using *Sonnet* and *AWR Microwave Office* software.

4.1 Circuit model for qubit

In order to build a circuit model out of discrete circuit elements one first has to obtain an element which models the physical qubit and its direct environment (ground plane, neighboring parts of resonator,
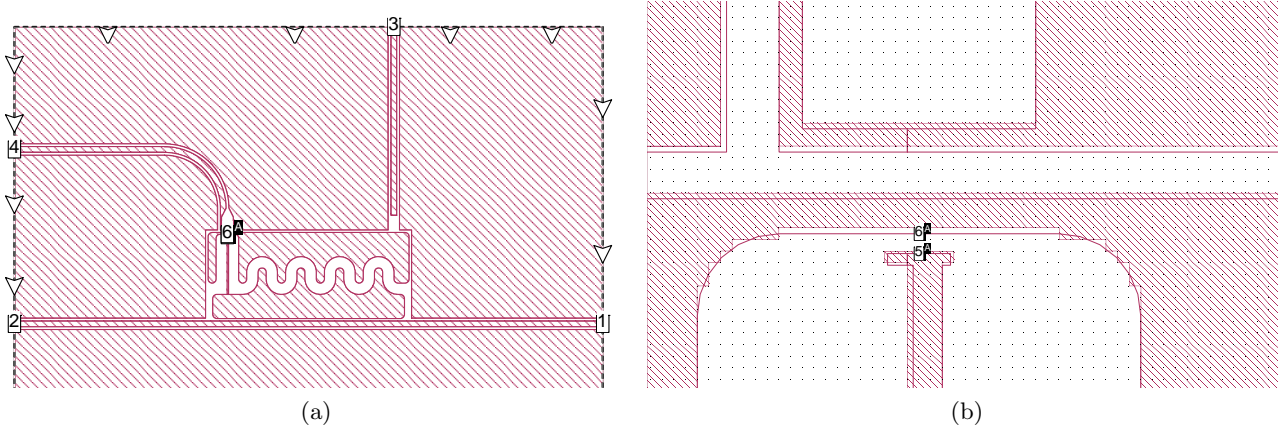
Figure 3: (a) Schematic of transmon qubit and its nearest environment in *Sonnet*. (b) Close-up view of Josephson junction. The two junctions have been removed and to each end a port (small white box) has been assigned.
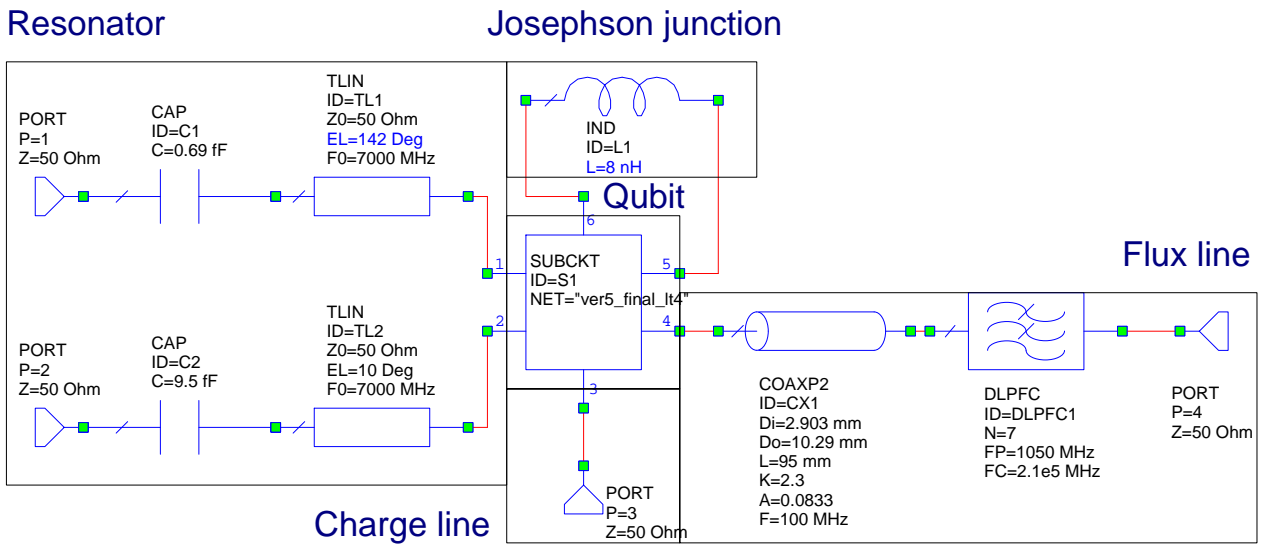

Figure 4: Schematic of circuit model in *AWR Microwave Office*.

charge- and flux line). This has been done using the software *Sonnet*. In Figure 3a a *Sonnet* project schematic of a the transmon qubit and its nearest environment can be seen. The qubit circuit is modelled as a flat, lossless metallic structure on top of a $500\,\mu$m thick sapphire substrate. This schematic is a cutout of the actual chip used in the experiment. To each control electrode (resonator, flux- and charge line) to which an external electrical signal can be applied a port has been assigned. These ports can later be used in a circuit design program to connect other circuit components to the qubit, modelling the control circuit. In order to have full control over the qubit frequency in the circuit model to be presented the two Josephson junctions have been removed as shown in Figure 3b and to either side of the qubit a port has been assigned (ports 5 & 6). *Sonnet* allows to simulate the transmission matrix (S-parameters) between the defined ports of the described circuit. The desired frequency range, interval size and accuracy for the simulation of the S-parameters can be specified. The results are stored as touchstone file format. The corresponding .s6p file can directly be imported as 6-terminal subcircuit into *AWR Microwave Office* .

4.2   Classical microwave circuit model

Starting from the qubit subcircuit obtained in *Sonnet* one can build a complete circuit model for the control circuit used to manipulate the qubit. Figure 4 shows the circuit schematic built in *AWR Microwave Office*. In the model the island and the reservoir of the qubit have been reconnected using

a lumped element inductor. By varying the inductance, the qubit frequency can be tuned as shown in Figure 5.

The resonator has been modelled by a lossless transmission (TL) line which is intersected by the qubit circuit. At in- and output the TL has been capacitively coupled to 50 Ohm ports. The qubit has been placed at one end of the resonator (achieved by choosing the transmission phase of one TL to be much larger than the phase of the other TL). The charge line has been modelled as a 50 Ohm port. For modelling the flux line a coaxial lossy transmission line, a low-pass filter and a 50 Ohm port was used. For the qubit subcircuit one has to provide the S-parameters for the desired frequency range. This 6×6 matrix (for every frequency point) can be simulated using an electromagnetic field solver like *Sonnet* (described above).

In a second step a two-terminal subcircuit, modeling an ecosorb filter, was inserted between transmission line and low-pass filter into the flux line. The S-parameter file for this subcircuit has been provided by measurements of the actual filters.

Figure 5: Qubit frequency as function of the inductance of the lumped element inductor. Dots correspond to frequencies obtained in *AWR Microwave office* and the solid line is a fit to the data using the expression for the frequency of an ideal LC-oscillator with a capacitance value of C_{fit}. Using electrostatic simulations to estimate the qubit capacitance one obtains C_{sim}.

4.3 Estimation of T_1

In order to get an estimate for the energy relaxation time T_1 the above described circuit model was used to simulate the transmitted power from port 1 to port 2 as function of the microwave frequency. At the qubit frequency the transmission spectrum has a sharp peak as shown in Figure 6a. The energy relaxation time was calculated as the resonance linewidth

$$T_1 = \frac{1}{4\pi\kappa}$$

where 2κ is the full width at half maximum of the qubit resonance. These line shapes have a Lorentzian profile. This allows to measure the linewidth by looking at the phase shift of the transmitted signal. At the qubit frequency the phase undergoes a shift by 180 degrees as shown in Figure 6b. The resonance width 2κ could then be extracted, due to the Lorentzian profile, by measuring the length of the interval between +45 and -45 degrees around the inflection point of the phase shift (see Figure 6b).
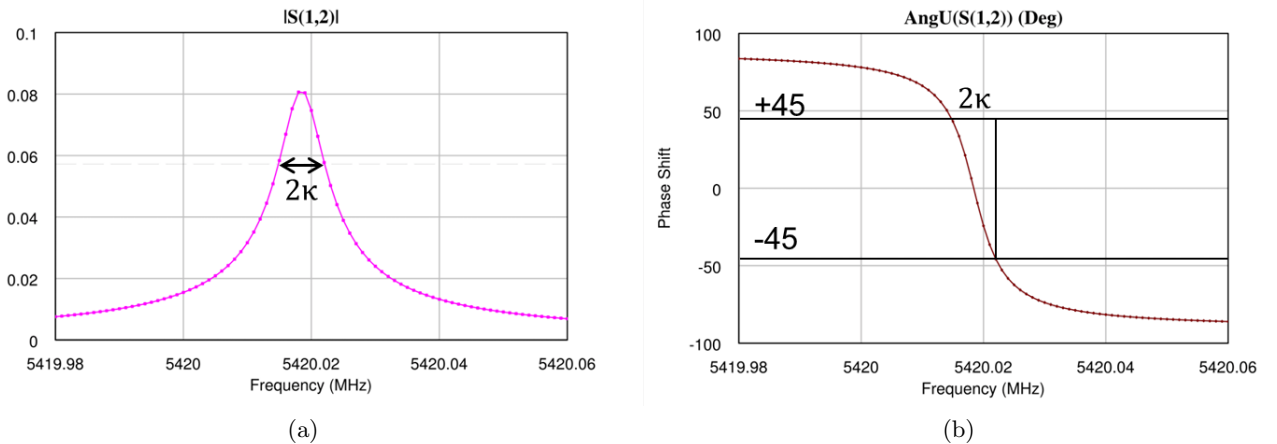

(a)

(b)

Figure 6: (a) Resonance in transmission spectrum (port 1 to port 2) at qubit frequency. (b) Linewidth of resonance can be extracted from the phase shift at the qubit frequency as explained in the text.
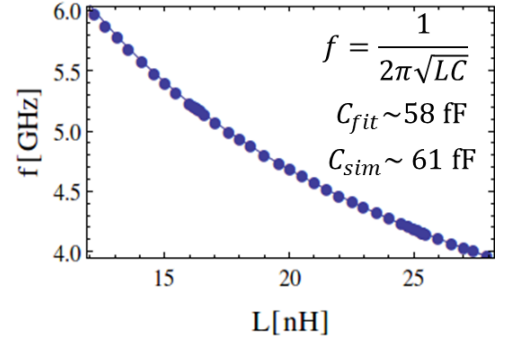
9

4.4 Estimation of relevant coupling parameters using Maxwell simulations

In the later stage of the semester project a new qubit design was developed. In order to estimate important qubit parameters electrostatic and magnetostatic simulations using the software *Maxwell* have been carried out. These simulations were done according to the procedure described in [16].

4.4.1 Magnetostatic simulations

In order to estimate the inductive coupling between the SQUID-loop and the flux line, the mutual inductance between these two has been simulated using the magnetostatic solver mode of *Maxwell*. This mode allows to define a static current excitation in each conductor loop. The program then solves for the electric and magnetic fields and calculates from these the inductance matrix of all defined current loops. With help of these simulations the optimal position and area of the SQUID-loop was determined. In Figure 8 a picture of the new symmetric design is shown.

4.4.2 Electrostatic simulations

The parameters E_c, E_J and g depend on the capacitance matrix of all the conductors in the qubit circuit. In Ref. [16] a model is presented to calculate these parameters from the capacitance matrix. In this model the island and the reservoir of the qubit are considered as separate conductors. Since the reservoir and the island are connected in the actual circuit one has to artificially cut the conductors for the electrostatic simulations. The cut between reservoir and island has been made at the two Josephson junctions, at the same place as in the *Sonnet* schematic presented above (cp. Figure 3b).

5 Results

5.1 Simulation old design

The above described circuit model has been used to simulate the energy relaxation time T_1 as function of qubit frequency ν for an actual qubit (qubit1 of mask 23 see Figure 3a). The results are shown in Figure 7a for the case without and in Figure 7b for the case with an ecosorb filter installed.

5.1.1 Without Ecosorb filter

In the first place the qubit has been simulated without taking the dielectric loss of sapphire into account. The corresponding T_1 trace is shown in red (squares) in Figure 7a.

The simulation reproduces qualitatively the resonant behavior of the measurements. This may be understood by considering the flux line as a resonator whose resonance frequency is determined by the total length of the flux line, which enters as a parameter into the model. In the simulation a total length of 95 mm has been used which matches the observed spacing of about 1 GHz between two neighboring resonances. The position of the resonances coincides not perfectly with the measurement, because the total length of the flux line, is only known with a precision of millimeters.
Off-resonance the simulated relaxation times are by one order of magnitude larger than in the measurements, indicating that some dominant decay process has not been taken into account.

In a second step energy relaxation due to dielectric loss has been simulated by specifying a non-zero dielectric loss tangent for the substrate material sapphire in the Sonnet simulations. The yellow and green trace corresponds to a dielectric loss tangent of $4 \cdot 10^{-6}$ and $5 \cdot 10^{-6}$ respectively. These values for the loss tangent are in agreement with Ref. [15], obtained by measuring the linewidth of an aluminum CPW resonator on a sapphire substrate at low temperatures and low intensities. The T_1 traces show significantly reduced values for energy relaxation.

5.1.2 With Ecosorb filter

In order to get rid of the resonant behavior of T_1, an ecosorb filter has been inserted before the low-pass filter (seen from qubit) into the flux line. The measurements (blue dots in Figure 7b) show a flattened T_1 trace and an overall reduction of relaxation time. In the AWR simulation the ecosorb filter has been included as a 2-terminal subcircuit, using the S-parameter data, obtained by measurements of
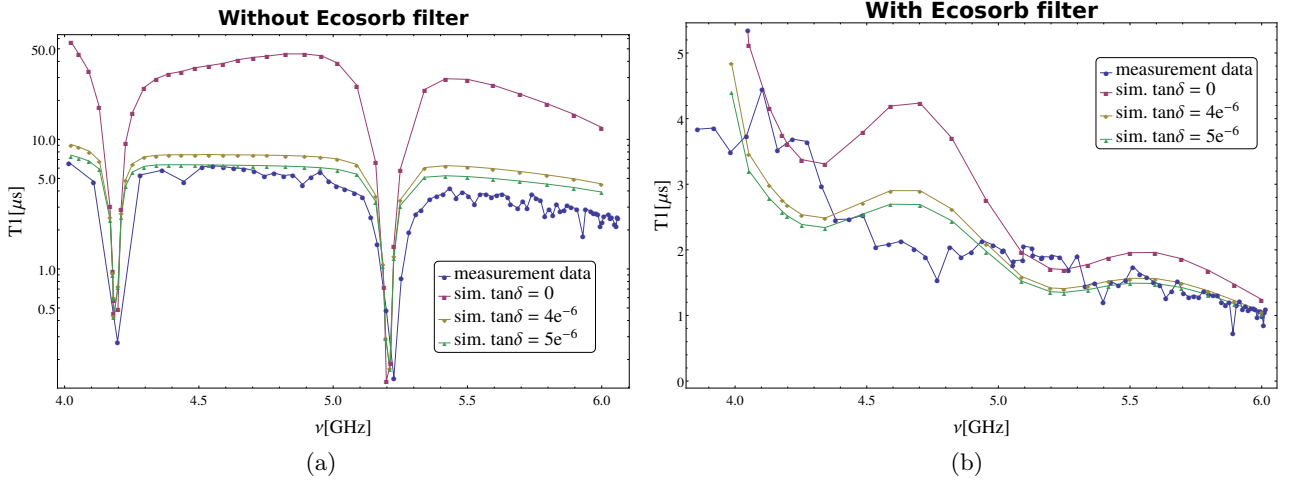
Figure 7: (a) T_1 versus ν for qubit 1 (Mask23). The measured relaxation times T_1 (blue circles) show resonance behavior, due to coupling of the qubit to the flux line which acts as a resonator. The red, yellow and green curve are simulated T_1 traces using the circuit model presented in the text. Including dielectric loss coming from the sapphire substrate T_1 times reduce significantly (yellow and green). (b) T_1 versus ν for qubit 1(Mask23) after insertion of Ecosorb filters into flux line. The filters flatten out the T_1 curve, while reducing the maximum values for relaxation times. The simulations (yellow and green) still show a slight resonance behavior.

the actual filter. In the first step the qubit has been simulated without taking dielectric loss into account, which lead to the red curve in Figure 7b. In a second step dielectric loss has been included by specifying a non-vanishing dielectric loss tangent for sapphire. The corresponding traces are given in yellow and green for values for the loss tangent of $4 \cdot 10^{-6}$ and $5 \cdot 10^{-6}$ respectively.

All simulated traces still show a slight resonant behavior which is not seen in the measurement data. Nevertheless, like in the case without an installed ecosorb filter using a dielectric loss tangent of the order of a few 10^{-6} gives reasonable T_1 estimates over a frequency range of $2\,\mathrm{GHz}$.

5.2   Proposed new design

Although the relaxation time seems to be limited by some internal decay channel like dielectric loss to around $10\,\mu s$ there is still some improvement possible, which we hope to achieve by changing to a more symmetric qubit and flux line design. For a perfectly symmetric qubit and flux line design the mutual inductance M' should vanish and the corresponding decay channel should not add any contribution to the total decay rate. A schematic of the new design can be seen in Figure 8. The design parameters have been chosen such that the coupling to the SQUID-loop M, E_C, E_J and g are similar to the old design. A list of simulated qubit-parameters for the old and the new design can be found in Table 1.
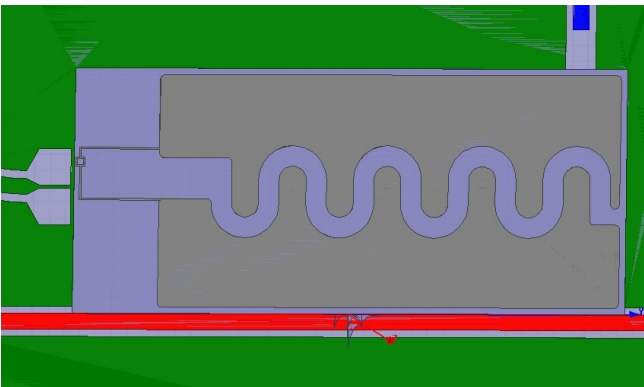

Figure 8: *Maxwell* schematic of the new qubit.

Table 1: Qubit parameters for the old and the new symmetric design

Parameter	Value [MHz]	
	old qubit	new qubit
E_c	300	306
g	260	216
E_j	20000	26150

5.2.1 T1 estimation

To estimate the energy relaxation time of the new design, it has also been simulated using the circuit model described above. The corresponding T_1 traces can be found in Figure 9. Depending on the values used for the dielectric loss tangent, we expect T_1 to be limited to $7\,\mu$s-$9\,\mu$s for the symmetric design. There are still some sharp resonances, which are believed to be present because of some residual mutual inductance M' due to the SQUID loop, which is shifted away from the symmetry axis of the flux line, making the new design not perfectly symmetric. Moreover the T_1 traces decay slower over frequency.
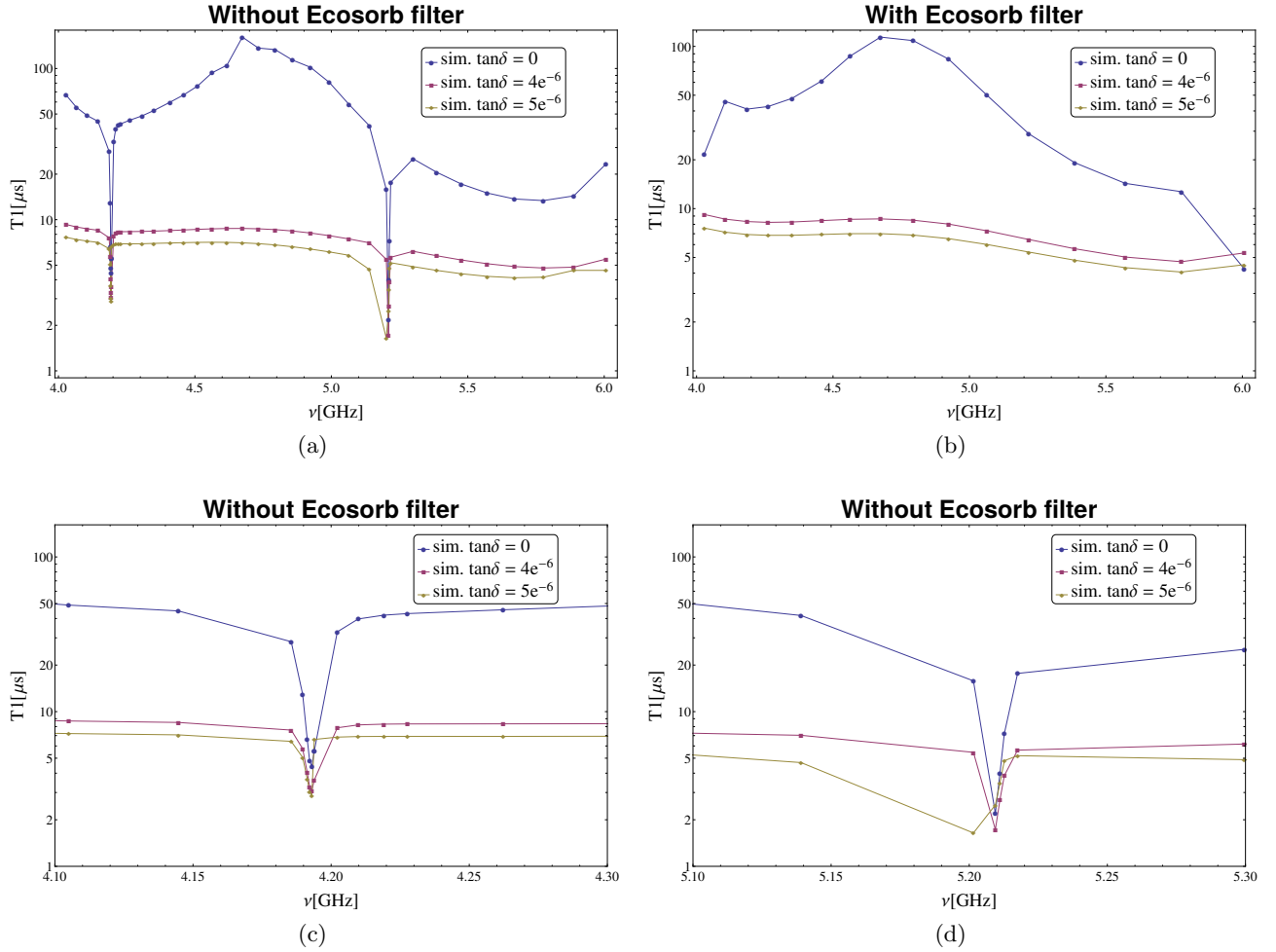

Figure 9: Simulated T_1 trace versus frequency ν for the new symmetric design, once for the case with (a) and once for the case without (b) an ecosorb filter installed. Traces (c) and (d) are blow-ups of trace (a) around resonances.
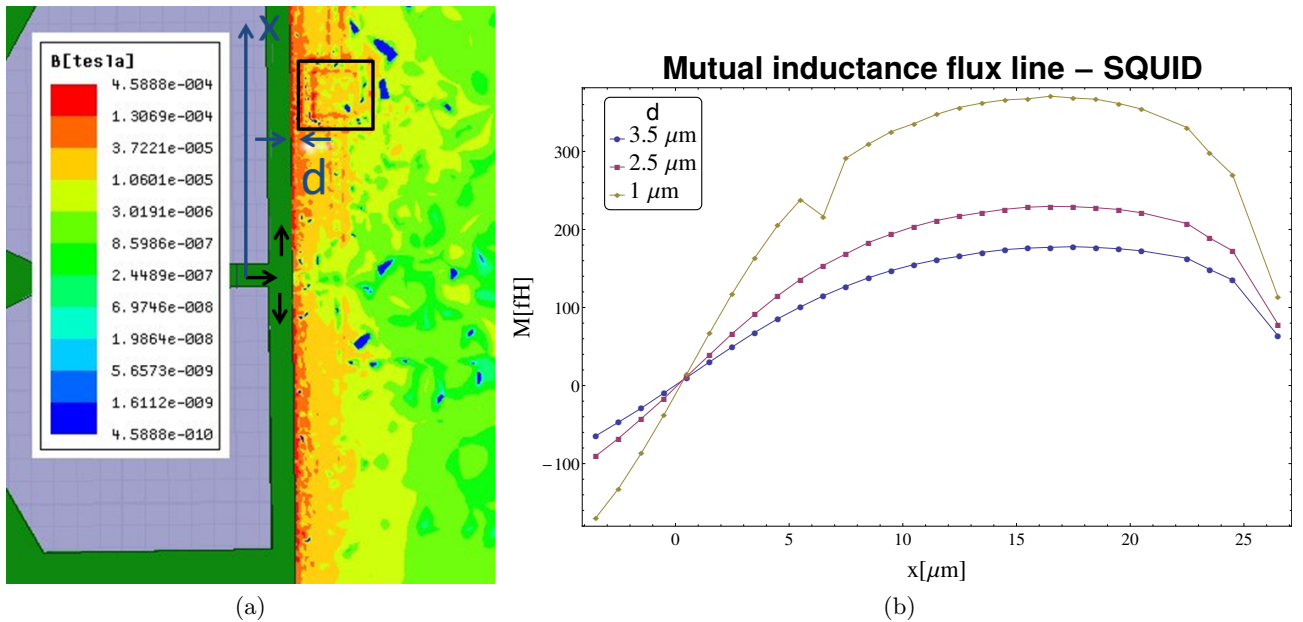
(a)   (b)

Figure 10: (a) Magnetic field distribution due to current flow in flux line (indicated by black arrows). For fixed separation d of the SQUID-loop (indicated by black box) from the flux line the B-field increases first with larger distance x from symmetry axis until it decreases again. (b) Mutual inductance between flux line and SQUID-loop as function of SQUID separation from symmetry axis.

5.2.2 SQUID-loop coupling to fluxline

In order to determine the optimal position and size of the SQUID-loop magnetostatic simulations in *Maxwell* have been made. In these simulations a static current has been defined in the flux line and the resulting coupling between SQUID and flux line has been simulated as function of position. Figure 10a shows the magnetic field distribution generated by a current flow of 1 mA in the flux line (direction of flow is indicated by arrows). For a SQUID positioned on the symmetry axis of the flux line the coupling vanishes. Keeping the separation d to the flux line fixed and moving the SQUID downwards increases the local B-field and thus the coupling before some maximal value is reached at a distance of about $-15\,\mu$m. Shifting the SQUID further downwards decreases the coupling again. Figure 10b confirms this qualitative explanation more quantitatively by plotting the inductive coupling versus the distance to the symmetry axes of the flux line for three different separation distances.

6 Discussion

The described circuit model reproduces qualitatively the resonance behavior of the measured T_1 trace for the case that dielectric loss is not included. On the other hand, the absolute T_1 values for the case without an ecosorb filter installed differ by one order of magnitude from the measurements. This indicates that some dominant decay process is not taken into account. We assume that multimode Purcell decay to the resonator and the flux line as well as decay to the charge line are captured by the described model. Under these considerations dielectric loss due to the substrate material sapphire seems to be one of the most prominent processes not taken into account. We included the effects of dielectric loss by specifying reasonable values for the dielectric loss tangent for sapphire in the simulations of the S-parameter matrix using *Sonnet*. Our results suggest that dielectric loss might be an explanation for the observed limited T_1 times.

7 Conclusion and Outlook

In conclusion a new classical microwave circuit model was presented which allows for quantitative estimations of the energy relaxation time T_1 as function of qubit frequency. The simulations using this model indicate that T_1 times are limited by some design unspecific process most probably dielectric

13

loss. Further measurements and simulations should be carried out to pin down the major decay process limiting T_1 which might eventually lead to a change in fabrication procedure and/or materials. In addition a new qubit design was proposed which should increase T_1 times by a factor of 2-3.

8   Acknowledgement

Appendix

A AWR Microwave Office 10 manual

A.1 General

In order to start a new project click on *File > New Project* . As a first step one should specify the units one wants to use throughout the project. For this double click on the *Project Options* in the Project tree on the left side of the window and go to the tab *Global units* and chose the desired units. In the left Project tree you can then right click on *Circuit Schematics* and select *New Schematic*. Switch to the *Elements* tab below the project tree. From these circuit elements you can build your circuit model. If you want to include a subcircuit specified by an S-parameter file you first have to import the data. For this right click on *Data File* in the project tree and select *Link to Data File* and browse for the desired data file. You can also import the data file, but in this case the data is not updated in your project if you change the external data file. Now click on *Subcircuit* in the top toolbar to add the imported data as a subcircuit to the current schematic. You have to select the data file which you want to use, *Microwave Office* then automatically creates a subcircuit with the right number of ports specified by the linked S-parameter file.

A.2 Making Graphs

If you have completed your schematic you can for example look at the transmission function of the circuit between two particular ports. In order to do so right click on *Graphs* and select *New Graph*. Then right click on the empty graph and select *Add New Measurement*. Under *Data Source File* select the desired Schematic. In order to plot the transmission function from port i to j: select *Port Parameters* in the submenu *Linear* in the *Measurement Type* box. In the *Measurement* box select S and on the right side of the window select the desired input and output measurements ports i and j. In the lower part of the window one can select which part of the complex transmission function one wants to plot. In order to specify the frequency range for plot double click on *Project Options* in the project tree go and to the *Frequencies* tab. There the frequency range and the step size can be chosen. For a given choice of frequency range click on *Apply* before clicking on *ok* otherwise the new frequency range will be discarded.

A.3 Measuring the linewidth

In order to measure the linewidth of a transmission resonance at a certain frequency one first has to tune the qubit to this frequency. This can be achieved by tuning the value of the inductance connecting ports 5 and 6. In order to do so go to the schematic and select the *Tune Tool* (blue screwdriver) in the top toolbar and click on the parameter value of the component you want to tune. Then go back to the graph and click on the *Tune* symbol (next to the Tune Tool symbol). In the appearing window you can vary the parameter value specified before by moving a switch up and down or by typing in the desired value. Now you can position the qubit resonance to the frequency of interest. Then you can zoom in by specifying a smaller frequency window around the resonance. The linewidth can be measured using markers. Click on *Add Marker* in the top toolbar and place the marker on the graph. Then right click on the marker and search for the desired value of the function left to the resonance. Repeat the same step searching the desired function value to the right side of the resonance. Now right click on one of the markers and select *Reference Marker* . The values for the other marker will now be given relative to the reference marker. In this way you can for example determine the FWHM of the transmission resonance.
When setting up the schematic for the first time one has to position the resonator resonance at the right frequency (determined by the simulated system). In order to do so one can tune the transmission phase of one transmission line, modelling the resonator, such that the second resonance, which is due to the resonator, is positioned at the exact resonator frequency.

B   Sonnet version 14.52 - Technical details and manual

B.1   General

In order to open a new file click on *File > New Geometry*. Before a new schematic is drawn or imported it is best to first specify the correct units and size of the later structure. Click on *Circuit > Units* and chose the desired units (for qubit design microns are suitable as length units) and check the box remember settings, such that you don not need to do this step a second time when you make a new schematic. In a second step click on *Circuit > Box* . In this window you can specify the cell size which is the size of the mesh boxes used for the simulation. The smaller the cell size the more accurate the simulation will be, but using too small cells will require too much memory. A typical value used was 0.5 or 1 micron. The cell size should be chosen such that the smallest feature size of the design is a multiple of the cell size. In the second row the total size of the whole circuit can be specified.

B.2   Drawing and Importing a Design, Layer settings, Ground connections

Sonnet allows to draw the entire structure to be simulated using polygons and other predefined shapes. For this click on *Tools > Add Metallization* and chose the desired shape.

Another way is to import a CAD drawing (e.g. as .dxf format) which has been exported from some other software (like *AutoCad* or *Maxwell*). For this click on *File > Import > DXF* and browse for the desired file. The entire structure needs to be fitted into the box which has been defined earlier and is shown by a solid black line.

The imported structure, denoted as "0"-level, is placed between two dielectric layers (shown as two green rectangles in the top left image). The two dielectric layers can be specified by double clicking on the corresponding image or by clicking on *Circuit > Dielectric Layers* and selecting the corresponding layer. In the appearing window click on *Select dielectric from library* and the desired dielectric can be chosen. For the lower dielectric sapphire and for the upper dielectric vacuum (which is the default setting) both with a thickness of 500 microns were used. In a second box the thickness of the layer can be specified. In order to include loss due to the substrate material one can specify magnetic and dielectric loss tangents for the chosen substrate in the lower part of the window. Magnetic and dielectric loss tangents have always been chosen symmetrically for all crystal directions.

By double clicking on a part of the structure one can specify the metal and the fill type. As we are simulating superconductors "Lossless" is a good choice for the metal. Using the fill type "Staircase" will produce the most accurate solution (which should be used for reliable results), as the other two types will use less memory.

Sonnet uses a common ground reference plane (denoted by *GND* in the layer schematic on the left-hand side) which is located below the lower dielectric layer. All ground planes in the design should be connected to this common ground. This can be achieved by placing so called *Edge Vias* which connect the different ground planes with the bottom of the Sonnect box over the side walls of the lower substrate. For placing a via click on *Tools > Add Via > Edge Via* and click on the edge of the ground plane you would like to connect to ground.

B.3   Ports

Ports have to be defined always on the edge of a polygon at locations were one later wants to connect other elements to the circuit. In our case these are the endpoints of resonator, charge and flux line and the two edges where the Josephson junctions have been removed. To add a port click on *Tools > Add Port* and place it on the desired polygon edge. By double clicking on a port the settings for this particular port can be chosen. All ports have been used with default values (e.g. 50 Ohms) with the exception of the port type. Ports in Sonnet can be grounded or co-calibrated. Ports 1 to 4 have been grounded, which means that the positive terminal is connected to the edge of a polygon (e.g. end of resonator or charge line) and the negative terminal is connected to ground. For doing so double click on the port and select "Autognd".

The two internal ports 5 and 6 are co-calibrated with floating ground, which means that the positive terminal is connected to the edge of a polygon (e.g. one end of Josephson junction) and the negative terminal is connected to a common ground, which is not connected (i.e. floating) to the reference ground of the entire structure to which ports 1-4 are connected to. This choice of port type is made according to the suggestion of the *Sonnet* manual [17], which recommends using co-calibrated ports for internal ports which are later connected to an element model which does not have a ground reference. Double click on the port and select "Co-calibrated" and then select "New A" for the name of the first co-calibrated port, click on *Properties* and select "Floating" for the "Ground Node Connection". For every further co-calibrated port with the same floating ground also choose "A" as "Name" in the "Calibration group" submenu.

B.4 Simulation Settings

Before the simulation can be started one has to define a few parameters. First one has to specify the frequency range. Click on *Analysis > Setup* . Select "Adaptive Sweep" in the "Analysis Control" submenu and specify the desired frequency range. Ensure that in the "Speed/Memory" menu the bar is positioned at the leftmost place. In the menu "Advanced" the number of points into which the frequency interval should be subdivided can be specified. For very accurate simulations 10000 points in a frequency interval of 10 MHz have been chosen (produces a 200 MB data file). For less accurate simulations 100000 points in an interval of 2GHz have been used.

As a last step go to *Analysis > Output Files* and click in the "Add File(s)" menu on *S,Y,Z Parameters*. Select "Touchstone" as file format and "S-Param" in the box "Parameters". Ensure that the box "High precision" is selected.

Now the simulation can be started. It makes sense to check first how much memory is used by the simulation. This can be done by clicking on *Analysis > Estimate Memory* . If the simulation requires too much memory one can make the cell size larger (which reduces the accuracy of the simulation) or cut out pieces of the structures which are not that important (e.g. large ground planes). For this use the "Reshape" command in the *Tools* menu and select the corner points of the structure you want to make smaller. You can then drag these points to the new desired location.

To run the simulation click on *Project > Analyze* . After the simulation has ran it will output the .s6p file in the specified output folder. This touchstone file can then be directly imported as a subcircuit into a circuit model program such as *AWR Microwave Office*.

C   Maxwell schematic

In figure 11 a *Maxwell* schematic of the qubit, with all important parameters that can be adjusted, is shown.
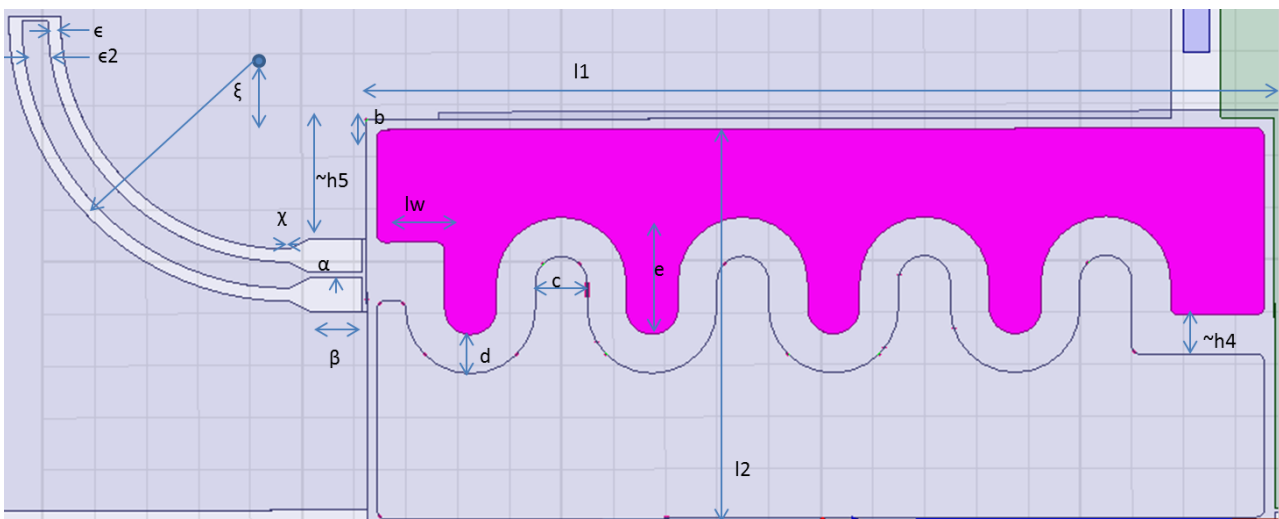

Figure 11: Important qubit parameters that can be changed in the *Maxwell* schematic.

D Declaration of originality

ETH

Eidgenössische Technische Hochschule Zürich
Swiss Federal Institute of Technology Zurich

Declaration of originality

The signed declaration of originality is a component of every semester paper, Bachelor's thesis, Master's thesis and any other degree paper undertaken during the course of studies, including the respective electronic versions.

Lecturers may also require a declaration of originality for other written papers compiled for their courses.

_____

I hereby confirm that I am the sole author of the written work here enclosed and that I have compiled it in my own words. Parts excepted are corrections of form and content by the supervisor.

Title of work (in block letters):

Qubit Simulation and Design

Authored by (in block letters):
For papers written by groups the names of all authors are required.

Name(s):
Ryser

First name(s):
Adrian

With my signature I confirm that
- I have committed none of the forms of plagiarism described in the 'Citation etiquette' information sheet.
- I have documented all methods, data and processes truthfully.
- I have not manipulated any data.
- I have mentioned all persons who were significant facilitators of the work.

I am aware that the work may be screened electronically for plagiarism.

Place, date
Zürich, 18. 12. 14

Signature(s)
Adrian Ryser

For papers written by groups the names of all authors are required. Their signatures collectively guarantee the entire content of the written paper.

References

[1] M. A. Nielsen and I. L. Chuang *Quantum Computation and Quantum Information* (Cambridge University Press, Cambridge, 2000).

[2] P. W. Shor SIAM J. Comp. **26** , 1484 (1997).

[3] L. K. Grover Phys. Rev. Lett. **79** , 325 (1997).

[4] Vandersypen, L. M. K. et al. Nature **414** , 883(2001).

[5] L. DiCarlo, J. M. Chow, J. M. Gambetta, Lev S. Bishop, B. R. Johnson, D. I. Schuster, J. Majer, A. Blais, L. Frunzio, S. M. Girvin and R. J. Schoelkopf Nature **460** , 7252 (2009).

[6] Michel H. Devoret and John M. Martinis *Implementing Qubits with Superconducting Integrated Circuits* Quant. Inf. Proc,**3** 163 (2004).

[7] D. Leibfried, R. Blatt, C. Monroe and D. Wineland *Quantum dynamics of single trapped ions* Review of Modern Physics **75** , 281 (2003).

[8] Pieter Kok, W. J. Munro, Kae Nemoto, T. C. Ralph, Jonathan P. Dowling, and G. J. Milburn *Linear optical quantum computing with photonic qubits* Rev. Mod. Phys. **79** , 135(2007).

[9] R. Barends, J. Kelly, A. Megrant, D. Sank, E. Jeffrey, Y. Chen, Y. Yin, B. Chiaro, J. Mutus, C. Neill, P. O'Malley, P. Roushan, J. Wenner, T. C. White, A. N. Cleland, and John M. Martinis PRL **111** , 080502 (2013).

[10] J. Koch, T. M. Yu, J. Gambetta, A. A. Houck, D. I. Schuster, J. Majer, A. Blais, M. H. Devoret, S. M. Girvin, and R. J. Schoelkopf, Phys. Rev. A. **76**, 042319 (2007).

[11] B. D. Josephson, Phys. Lett. **1**, 251 (1962).

[12] E. M. Purcell Phys. Rev. **69**, 681 (1946).

[13] A. A. Houck, D. I. Schuster, J. M. Gambetta, J. A. Schreier, B. R. Johnson, J. M. Chow, J. Majer, L. Frun- zio, M. H. Devoret, S. M. Girvin, and R. J. Schoelkopf, cond-mat/0702648 (2007).

[14] Robert McDermott *Materials Origins of Decoherence in Superconducting Qubits* IEEE TRANS-ACTIONS ON APPLIED SUPERCONDUCTIVITY, **VOL. 19** , NO. 1(2009).

[15] Aaron D. O'Connell, M. Ansmann, R. C. Bialczak, M. Hofheinz, N. Katz, Erik Lucero, C. McKenney, M. Neeley, H. Wang, E. M. Weig, A. N. Cleland, and J. M. Martinis, APL **92**, 112903 (2008).

[16] Simon Burkhard, *Optimization of transmon design for longer coherence time*, Semester Thesis, ETH Zürich, 2012.

[17] *Sonnet® User's guide*, Release 12, 2009.